

International Journal of Exergy

ISSN online: 1742-8300 - ISSN print: 1742-8297

<https://www.inderscience.com/ijex>

Energy and exergy analysis of two solar-geothermal assisted biomass-driven hybrid cycles to produce power, heat, and distilled water

Maliheh Pashapour

DOI: [10.1504/IJEX.2024.10062054](https://doi.org/10.1504/IJEX.2024.10062054)

Article History:

Received:	08 September 2023
Last revised:	17 December 2023
Accepted:	17 December 2023
Published online:	01 February 2024

Energy and exergy analysis of two solar-geothermal assisted biomass-driven hybrid cycles to produce power, heat, and distilled water

Maliheh Pashapour

Department of Mechanical Engineering,
Naghadeh Branch,
Islamic Azad University,
Naghadeh, Iran
Email: m.pashapour@urmia.ac.ir

Abstract: In this article, the solar and geothermal energies strengthen the proposed cycles A and B. The base of both is the biomass-driven gas turbine-organic Rankine combined cycle. A solar cycle with flat plate collectors preheats the ORC. The system B also has a geothermal cycle, which reheats the ORC, makes water steam, and runs a steam turbine. So, the system B produces 2,179 kW and 8.541 kg/s more power and water vapour, respectively. A reverse osmosis purification unit is attached to the end of each system. The required power of high-pressure pump is respectively supplied by the organic turbine and steam turbine in systems A and B which leads to the production of 35.83 kg/s and 83.09 kg/s distilled water by them. Overall, the energy and exergy efficiencies, and the exergy destruction of the system B is 111.3%, 49.32%, and 23.73% higher than system A, respectively.

Keywords: energy; exergy; biomass-driven gas turbine; geothermal assisted hybrid cycle; flat plate solar collector; reverse osmosis.

Reference to this paper should be made as follows: Pashapour, M. (2024) 'Energy and exergy analysis of two solar-geothermal assisted biomass-driven hybrid cycles to produce power, heat, and distilled water', *Int. J. Exergy*, Vol. 43, No. 1, pp.40–58.

Biographical notes: Maliheh Pashapour received her BS in Mechanical Engineering in 2006 from the Urmia University, Urmia, Iran. She received her Master's in Mechanical Engineering from the Urmia University, Urmia, Iran, in 2008. She received her PhD in Energy Conversion from the Urmia University, Iran, in 2019. Currently, she is working as an Assistant Professor in the Islamic Azad University, Naghadeh branch. Her research interests are combined energy conversion systems, multi-generation power plants, thermodynamic and economic analyses, heat transfer, and renewable energies.

1 Introduction

The rapid growth of population coupled with the lack of fossil resources and the problems of air pollution, climate change, and global warming are issues that prove the need to recover wasted heat and use renewable and clean energy sources. Helping to mitigate global warming and sustainability are among the reasons for the popularity of biomass (Cao et al., 2020). Asgari et al. (2020) have proposed a CCHP, including a gas

turbine based on biomass gasification, a heating unit, along with an absorption refrigeration cycle. They have analysed the system from an energy and exergy perspective. In the system studied by Musharavati et al. (2022), a heat exchanger uses the waste heat of the gas turbine open cycle with biomass drive to produce steam that is employed in a multi-effect purification unit. The system has been analysed thermodynamically and thermo-economically. It also optimised with the method of multi-objective grey wolf algorithm.

Among renewable sources are geothermal and solar energies. They can be used more effectively when combined with fossil fuel-based power plants and improve system efficiency. However, the ORC is a key and common technique to exploit them. Ochoa et al. (2023), in a particular area in Colombia with high solar radiation potential, thermo-economically and environmentally optimised two organic Rankine cycles driven with a flat plate solar collector and conducted a parametric study hourly basis using key parameters. An energy/exergy/exergy-economic/exergy-environmental study of a solar-geothermal CCHP compound system has been conducted by Alibaba et al. (2023). Aghaziarati and Hajizadeh Aghdam (2020) have proposed a combined solar-ORC system with a cascade refrigeration cycle for the power supply, cooling, and heating of a hospital. They have analysed this system from the point of view of energy, exergy, and exergy-economics. Bet Sarkis and Zare (2018) offered two solar-biomass compound cycles and compared them with each other as well as with another basic biomass-based cycle without solar energy. They analysed the systems in terms of Thermodynamic and economic. In the system investigated by Zhang et al. (2023), a double-flash geothermal cycle that is first indirectly heated by the solar system is the upstream cycle, and an ORC and an ejector refrigeration form the downstream cycles. They optimised the system using both energy-economic and exergy-economic ways. According to Altayib and Dincer (2022), a high-cost thermal storage system must be employed to use solar energy. So, they combined solar energy with geothermal energy in their approach, which includes a flash Rankine power plant, an ORC, and a heat recovery unit. They investigated three different configurations for the ORC with varying working fluids. The result is that the integration of the two mentioned energies is more effective than the independent use of each of them. Mohammadi et al. (2023) have simultaneously used solar and geothermal energies to drive the combination of a steam Rankine, an ORC, an ejector refrigeration system, a thermoelectric generator unit, and a reverse osmosis (RO) purification unit. They have analysed the mentioned system in terms of thermodynamics and economics and then optimised it based on the unit cost of components and exergy efficiency.

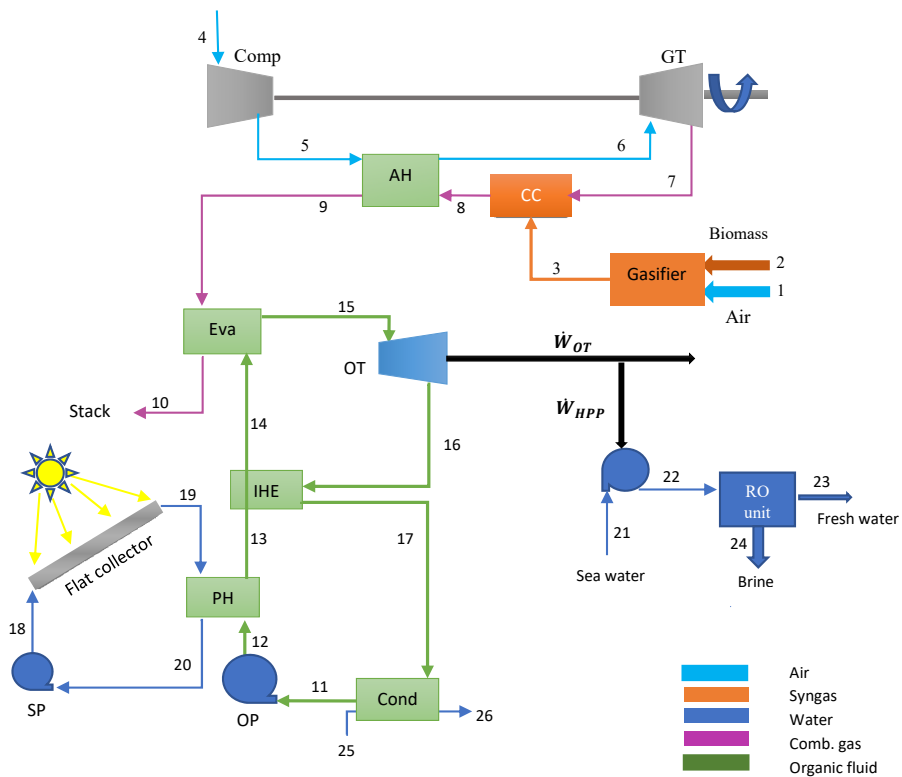
In this article, two multigeneration systems A and B, are analysed from an energy and exergy perspective and compared in terms of output parameters. In both systems, an organic Rankine cycle that recovers the exhaust heat of a biomass-based gas turbine cycle is preheated by a solar cycle. Solar collectors are the flat plate type. System B also has a geothermal cycle, that its energy reheats the organic Rankine cycle, produces steam in a steam generator, and runs a steam turbine to generates additional power. In the hybrid cycles mentioned in the literature, the combination of biomass with solar and geothermal energies has been analysed, but the share of each geothermal and solar energy on system output parameters has not been investigated. In this article, the contribution of these energies compared to the input biomass energy is determined and it is analysed which one has a greater effect to strengthen the ORCs that are employed for the high temperature waste heat recovery. A RO desalination unit is connected to end of the both

systems, whose high-pressure pump in system A and B consumes a part of the power of the organic turbine and steam turbine, respectively. The produced power by the geothermal turbine and consequently the distilled water by system B is much more. The effect of changing the key variables on the output parameters like power, distilled water, water steam, and energy and exergy efficiencies is investigated.

2 System description

Two proposed systems A and B, respectively shown by Figures 1 and 2, are here explained.

Figure 1 Layout of proposed biomass-forced compound system assisted by solar energy; system A (see online version for colours)



2.1 System A

Figure 1 shows the configuration of system A, a combined cycle consisting of a biomass-driven gas turbine and an ORC supported by a solar cycle. In this system, biomass and air with ambient temperature and pressure are fed to the gasifier. Produced synthesis gas (stream 3) is directed to the combustion chamber, then it burns as fuel with the high-temperature air coming from the GT (stream 7). The hot combustion gas (stream 8) goes thru the air heater and heats the high-pressure air leaving the compressor

2.2 System B

Figure 2 suggests the combined system B, whose biomass-fed gas turbine cycle is similar to system A, and its organic Rankine cycle is reinforced by the geothermal cycle in addition to the solar cycle. Geothermal energy is first used to reheat the organic fluid before entering the low-pressure turbine and then goes to the steam generator (stream 24) to produce saturated water steam (stream 28). The geofluid goes toward a steam turbine for power generation. Some of the power produced by this geo-turbine is consumed by the high-pressure pump of the RO desalination unit connected to the system. Finally, the fluid passes thru a condenser and a pump to reinject.

The assumptions for modelling the proposed multigeneration systems are as follows:

- The whole system remains in a steady state.
- The adiabatic compressor and gas turbine are employed.
- The combustion gas and air behave in the character of an ideal gas.
- The heat exchangers of the ORC and geo cycle have no pressure drop.
- Heat loss of the gasifier and combustion chamber, respectively are 5% and 2% of the total chemical energy of fuel (Asgari et al., 2020; Pashapour et al., 2019).

The data for modelling and simulating the mentioned systems are written in Table 1.

Table 1 The input data for systems modelling

<i>Parameter</i>	<i>Value</i>
Ambient temperature (K)	298.15
Ambient pressure (kPa)	101.3
GT	
Gas turbine/air compressor's isentropic efficiency (%)	89/87
Air compressor's pressure ratio (-)	10
Gas turbine inlet temperature (K)	1,400
Pressure drop in the combustion chamber (%)	3
Pressure drop in the cold/ hot side of the air preheater (%)	3/1.5
Pressure drop of flue gas in the evaporator (%)	2
Biomass moisture content by mass (%)	20
Gasification temperature (K)	1,073
Stuck temperature (°C)	180
Solar cycle	
Average solar radiation (kW/m ²)	0.800
The optical efficiency of the collector (η_{opt}) (%)	77
Linear heat loss coefficient (c_1) (kW/m ² K)	3.75×10^{-3}
Quadratic heat loss coefficient c_2 (kW/m ² K ²)	0.015×10^{-3}
Minimum temperature difference (pinch point) within the PH	10
The temperature of the sun (K)	5,770

Source: Bet Sarkis and Zare (2018), Bellos et al. (2021), Cen et al. (2021), Pashapour et al. (2021) and Nafey and Sharaf (2010)

Table 1 The input data for systems modelling (continued)

<i>Parameter</i>	<i>Value</i>
ORC	
Maximum temperature of ORC (°C)	150–250
Temperature of condenser (°C)	30–60
Isentropic efficiency turbines/pump (%)	85/85
Heat exchangers effectiveness (-)	0.85
Minimum temperature difference (pinch point) within the reheater/condenser	10/10
Geothermal cycle	
Geothermal temperature (K)	448.2
Geothermal pressure (kPa)	7,000
Geothermal mass flow rate (kg/s)	83
Isentropic efficiency turbine/pump (%)	85/90
Temperature of condenser (°C)	40
RO parameters	
Feed-water salinity [ppm]	45,000
Recovery ratio	0.3
Feed-water flow rate [m ³ /h]	486
Salt rejection (SR)	0.9944
Fouling factor (FF) [%]	85

Source: Bet Sarkis and Zare (2018), Bellos et al. (2021), Cen et al. (2021), Pashapour et al. (2021) and Nafey and Sharaf (2010)

3 Thermodynamic modelling

3.1 Energy analysis

Knowing that \dot{W} (kW) and \dot{Q} (kW) are respectively related to the rate of work and heat transfer from the boundaries of a control volume to the environment, the energy balance is (Pashapour et al., 2021):

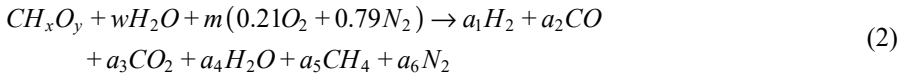
$$\dot{Q}_{C.V} + \sum_{in} \dot{m}_i h_i = \dot{W}_{C.V} + \sum_{out} \dot{m}_e h_e \quad (1)$$

where \dot{m} $\left(\frac{kg}{s}\right)$ and h $\left(\frac{kJ}{kg}\right)$ are the mass flow rate and specific enthalpy, respectively.

indices i and j are for input and output streams, respectively. In addition, energy analysis for the gasifier, combustion chamber, RO desalination unit, and solar collector are as follows in detail.

3.1.1 Gasifier

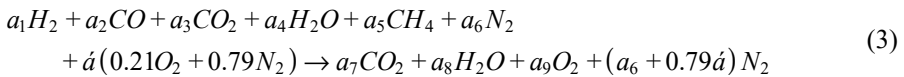
A downdraft kind of gasifier with four areas of drying/pyrolysis/reduction/and combustion is used in this paper. All reactions are in the chemical equilibrium. Also, before leaving the gasifier, the pyrolysis products reach equilibrium in the reduction zone (Bet Sarkis and Zare, 2018). The biomass is wood with the chemical formula of $CH_{1.44}O_{0.66}$ and chemical composition of C: 50%, H: 6%, and O: 44%; other contents like N and S are neglected. Equation (2) expresses the global gasification reaction (Asgari et al., 2020):



where $w(-)$ is the biomass moisture content. Seven unknown coefficients of a_1 to a_6 and m need seven equations. Mole balances for hydrogen, oxygen, carbon, and nitrogen consist of four of seven. At a certain temperature, energy equilibrium for the gasification process is one other equation. The equilibrium constants of the two reactions, i.e., water-gas shift and methane formation in the gasifier, are the last two equations of the seven (Asgari et al., 2020).

3.1.2 Combustion chamber

Between the entering air to the CC (with kilomoles of \dot{a}) and the syngas as fuel, complete combustion can be presented as equation (3) (Asgari et al., 2020):



3.1.3 Solar collectors

A flat plat kind of solar collector is considered in this paper. Its thermal efficiency (η_{col}) in terms of the optical efficiency (η_{opt}), and heat losses coefficients (c_1, c_2) (kw/m^2K) provided by the manufacturer, is expressed as (Aghaziarati and Hajizadeh Aghdam, 2020):

$$\eta_{col} = \eta_{opt} - c_1 \left(\frac{T_{col,m} - T_0}{G} \right) - c_2 G \left(\frac{T_{col,m} - T_0}{G} \right)^2 \quad (4)$$

where $T_{col,m}$ (K) is the mean temperature between the inlet and outlet of the collector. Knowing that G (kw/m^2), and A_{col} (m^2) are the solar irradiation and total surface of collectors, respectively, the useful thermal power ($\dot{Q}_u(kW)$) that solar fluid inside the collector can gain from the solar energy is $\eta_{col} \times G \times A_{col}$.

3.1.4 RO desalination unit

For the thermodynamic modelling of the desalination unit, the empirical energy equations are used (Nafey and Sharaf, 2010). Suppose $\dot{V} \left(\frac{m^3}{h} \right)$ and X (ppm) are the volume flow

rate and salinity of seawater, respectively, and the indices f , d and b are related to feed water, fresh water and brine, respectively. Net pressure difference through the membrane ΔP_{net} (kPa) can be achieved by equation (5):

$$\Delta P_{net} = \frac{\dot{V}_d}{3,600 \times TCF \times FF \times A_e \times n_m \times n_v \times k_w} + 37.92(X_f + X_b) - 75.84 \times X_d \quad (5)$$

where $FF(-)$, $A_e(\text{m}^2)$, $nm(-)$ and $nv(-)$, are the fouling factor, area of elements, number of membrane, and number of pressure vessels, respectively. TCF , and k_w (kW) are the temperature correction factor, and water permeability of the membrane, respectively.

$$TCF = \exp \left[2,700 \times \left(\frac{1}{T} - \frac{1}{298} \right) \right] \quad (6)$$

$$k_w = \frac{6.84 \times 10^{-8} \times (18.6865 - 0.177 \times X_b)}{T} \quad (7)$$

where T is temperature in (K). For more details, refer to our previous work (Pashapour et al., 2021). Power consumption of the high-pressure pump of the desalination unit is a part of ORC's turbine and geothermal steam turbine for systems A and B, respectively:

3.1.5 Energy efficiency

The energy efficiency of two proposed systems is defined as:

$$\eta_A = \frac{\dot{W}_{net,A} + \dot{m}_{d\gamma}}{(\dot{m} \times LHV)_{biomass} + \dot{Q}_u}; \dot{W}_{net,A} = \dot{W}_{GT} - \dot{W}_{AC} + \dot{W}_{OT} - \dot{W}_P - \dot{W}_{SP} - \dot{W}_{HPP} \quad (8)$$

$$\eta_B = \frac{\dot{W}_{net,B} + \dot{Q}_{SG} + \dot{m}_{d\gamma}}{(\dot{m} \times LHV)_{biomass} + \dot{Q}_u + \dot{m}_{23}(h_{23} - h_{26})}; \dot{W}_{net,B} = \dot{W}_{GT} - \dot{W}_{AC} + \dot{W}_{HPT} + \dot{W}_{LPT} - \dot{W}_P - \dot{W}_{SP} + \dot{W}_{GeoT} - \dot{W}_{HPP} \quad (9)$$

where $(\dot{m} \times LHV)_{biomass}$ is the biomass energy at the gasifier temperature $\left[\dot{m}_{biomass} \left(\frac{\text{kg}}{\text{s}} \right) \right]$ and $LHV_{biomass}$ (kJ/kg) are the mass flow rate and lower heating value of the biomass, respectively]. $\dot{m}_d \left(\frac{\text{kg}}{\text{s}} \right)$ and $\gamma \left(\frac{\text{kJ}}{\text{kg}} \right)$ are the mass flow rate and latent heat of distilled water, respectively. \dot{Q}_{SG} (kW) is the heat can be obtained in the steam generator ($\dot{Q}_{SG} = \dot{m}_{27}(h_{28} - h_{27})$).

3.2 Exergy analysis

Ignoring the potential and kinetic exergy changes, the exergy of each stream consists of two types, physical and chemical. The specific physical exergy of a defined state and the chemical exergy of an ideal gas mixture can be specified as equations (10) and (11), respectively (Pashapour et al., 2021):

$$ex^{ph} = h - h_0 - T_0 (s - s_0) \quad (10)$$

$$\overline{ex}_{mixture}^{ch} = \sum_i x_i \overline{ex}_{0,i}^{ch} + \overline{R}T_0 \sum x_i \ln x_i \quad (11)$$

where ex (kJ/kg) is the specific exergy and $\dot{m} \left(\frac{kg}{s} \right)$ is the mass flow rate. Index 0 symbolises the amount of a parameter in environmental conditions. And $x_{ki}(-)$ and $\overline{ex}_i^{ch} \left(\frac{kJ}{kmol} \right)$ are the mole fraction and chemical exergy per mole of component i of gas mixtures, respectively. The biomass chemical exergy is expressed as (Musharavati et al., 2022):

$$\overline{ex}_{biomass}^{ch} = \beta \times \overline{LHV}_{biomass} \quad (12)$$

where β is the ratio of exergy to $\overline{LHV} \left(\frac{kJ}{kmol} \right)$ of biomass and for solid fuels can be obtained by equation (13):

$$\beta = \frac{1.04 + 0.016 \frac{M_H}{M_C} - 0.34493 \frac{M_O}{M_C} \left(1 + 0.0531 \frac{M_H}{M_C} \right)}{1 - 0.4124 \frac{M_O}{M_C}} \quad (13)$$

where M_O , M_H , and M_C are the oxygen, hydrogen, and carbon mass fractions in the biomass, respectively. The solar exergy rate is $\dot{Ex}_{Solar} = GA_{col} \left[1 + \frac{1}{3} \left(\frac{T_0}{T_{sun}} \right)^4 + \frac{4}{3} \left(\frac{T_0}{T_{sun}} \right) \right]$.

According to the exergy balance for a control volume, the exergy destruction rate can be calculated by subtracting the loss and product exergies from the fuel exergy. Besides, the ratio of product exergy to the fuel exergy in each part forms the exergy efficiency of that part (Asgari et al., 2020).

3.2.1 Exergy efficiency

To investigate the sustainability of systems and their efficiency in using the energy sources as fuel, the exergy efficiency is provided. The overall exergy efficiency of the systems can be defined as the ratio of the output products exergy to the entire input exergy of fuels. The products of the system A are the power and distilled water with the fuel of biomass and solar energies. System B has three products of power, water steam and distilled water which are produced by spending biomass, solar and geothermal energies. The exergy efficiency of systems A and B can be obtained by equations (14) and (15), respectively:

$$\varepsilon_A = \frac{\dot{W}_{net,A} + \dot{Ex}_{23}}{\dot{Ex}_{biomass} + \dot{Ex}_{Solar}} \quad (14)$$

$$\varepsilon_B = \frac{\dot{W}_{net,A} + \dot{E}x_{23} + (\dot{E}x_{28} - \dot{E}x_{27})}{\dot{E}x_{biomass} + \dot{E}x_{solar} + \dot{E}x_{23} - \dot{E}x_{26}} \quad (15)$$

where $\dot{E}x$ is the exergy in kW.

4 Results and discussion

The engineering equation solver (EES) software (<http://www.fchart.com/ees/>) is employed to simulate the proposed systems.

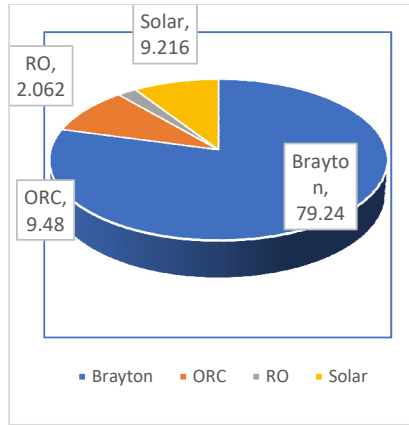
4.1 Numerical results

A comprehensive comparison of two mentioned systems outputs, based on the available data in Table 1, is illustrated. As known, for a given amount of biomass input, system B is more efficient than system A. Respectively, for systems A and B, the energy efficiency is 32.95% and 69.65%; and the exergy efficiency is 29.66% and 44.29%. It is due to the use of geothermal energy to reheat the organic Rankine cycle, and, more importantly, to obtain steam in the steam generator, as well as the presence of a steam turbine to use the remaining geothermal energy for generating more power. Net output power of system A and B is 6,272 kW and 8,444 kW, respectively. Further, system B produces 8.541 kg/s saturated water vapour that system A cannot. In addition, because in systems A and B, the RO pump consumes a part of the production power of the ORC's turbine and the geothermal turbine, respectively, and the geothermal turbine generates more power; therefore, more fresh water, 83.09 kg/s, is produced by system B; while system A makes 35.83 kg/s distilled water.

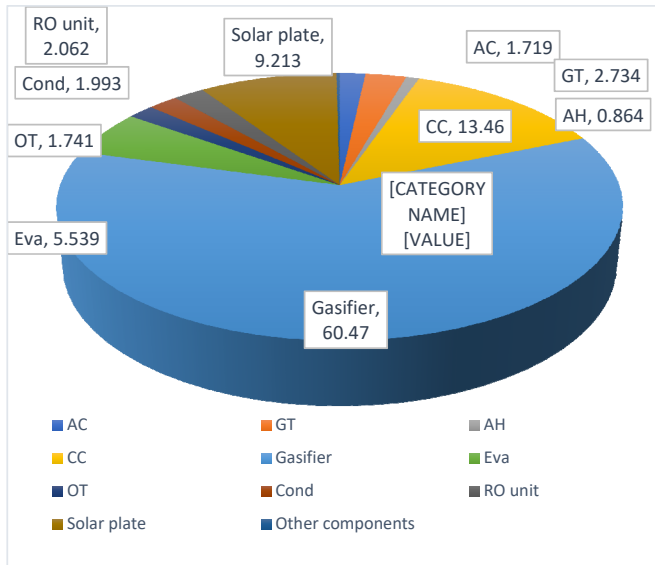
According to the obtained results, the geothermal source with high energy is very effective for improving the organic Rankine cycle, which is employed to recover the high-temperature waste heat of the gas turbine cycle. In contrast, the solar cycle with flat plate collectors can only be used for the preheating of such a cycle, because with its low temperature and mass flux, it cannot be more effective in the ORC. It seems that using a solar cycle with larger panels, other operating fluids, or other types of collectors, such as parabolic through collectors and solar dish collectors (Loni et al., 2021), which can produce higher temperatures, are more appropriate to strengthen the cycles used for high energetic waste recycling. It should be noticed that, as these methods increase the outlet temperature, they also impose more exergy destruction to the system and have a negative effect on the system efficiency, which should be considered. In the study conducted by Bet Sarkis and Zare (2018) (mentioned in the literature), the share of solar energy with parabolic trough collectors compared to biomass energy in one of the proposed configurations (configuration 1) was reported as 8.42%. In that cycle, solar energy was used to preheat the Rankine cycle. In another configuration (configuration 2), they increased the share of solar energy to 34.56% by adding 467% of the plate area and used it in another way. As a result, the output power of the cycle increased by 24.5% and the CO₂ emission decreased by 19.5%; but, due to the high exergy destruction of solar panels, the energy and exergy efficiencies decreased by 10.96% and 5.96%, respectively.

In the present work, the energy supplied through the solar cycle with flat plate collectors and water as the working fluid is about 4% of biomass energy for both systems and can only preheat the ORC. While, the energy that geothermal cycle gives to combined system B is 134% of biomass energy. Although, due to the presence of components such as a steam generator and geo turbine in the composition of the geothermal cycle, the system B destroys 23.73% more exergy than system A. Still, on the other hand, it causes a considerable increase in power production, fresh water, and water steam, as well as the energy/ exergy efficiencies by 34%, 132%, 100%, 111.3%, and 49.32%, respectively.

Figure 3 The exergy destruction shares for (a) each cycle, (b) each component of system A (see online version for colours)



(a)



(b)

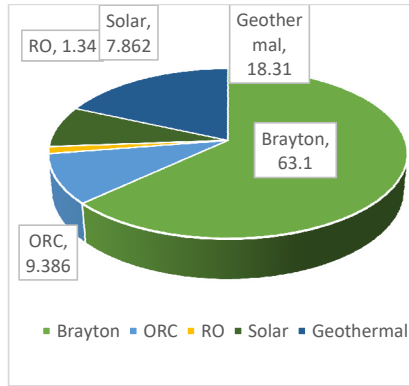
The contribution of each cycle and each component in the exergy destruction of system A is shown in Figures 3(a) and 3(b), respectively. According to these figures, the share of the Brayton cycle to the exergy destruction is 79.24%, much more than other cycles. The reason is the components such as the gasifier in this cycle, which alone accounts for 60.47% of the overall exergy destruction of the system A, followed by the combustion chamber with a share of 13.46%. The ORC and the solar cycle play an almost equal role in the exergy destruction of system A, because although the number of components of the organic Rankine cycle is more, the solar plate has a high exergy destruction. The RO unit has the most minor role in the exergy destruction of system A, with a share of 2%. Likewise, the contribution of each cycle and each component of system B in the exergy destruction rate of this system is shown in Figures 4(a) and 4(b), respectively. As seen, the Brayton cycle still plays the most prominent role in the exergy destruction. The reason is that 50.11% of the entire exergy destruction of this system is attributed to the gasifier used in this cycle. After that, the largest share of exergy destruction is related to the geothermal cycle, due to the presence of a steam generator and a geothermal condenser in it. The organic Rankine cycle, solar cycle, and the RO desalination unit are ranked third to fifth.

4.2 Parametric study

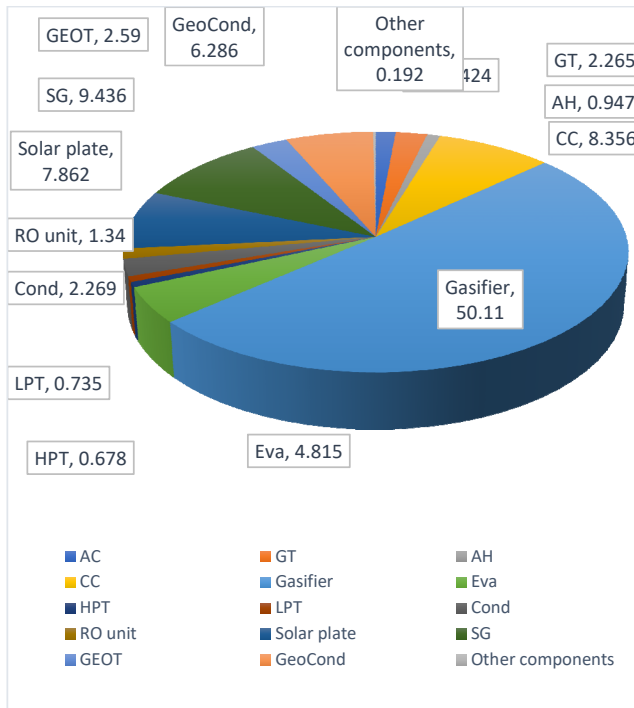
The behaviour of the offered systems under the varying of their fundamental design parameters is investigated. The response of those systems is evaluated in terms of energy/exergy efficiencies, net output power, amount of purified water, and exergy destruction. It should be noted that the effect of changes in one variable is studied by keeping other variables constant, according to Table 1.

One of the essential parameters whose change affects the behaviour of the proposed systems is the gas turbine inlet temperature. There are several ways to raise the gas turbine inlet temperature. One of them, according to Musharavati et al. (2022), is to increase the mass flow rate of biomass that results an increase in the mass flow and temperature of the air entering the gas turbine, and consequently its output power. On the other hand, the increase in the inlet temperature of the gas turbine is the result of absorbing more energy (heat) from the combustion gases by the air in the air heater. This means reducing the Brayton cycle exhaust energy to be recovered by lower cycles, if any. In another method that Bet Sarkis and Zare (2018) have stated, the mass flow rate of biomass is constant and by reducing the mass flow rate of air from the compressor to the air heater, they increase the inlet temperature of gas turbine. In this case, the output power of the gas turbine as well as the temperature of the Brayton cycle exhaust gases increases. In the first method, the gas turbine experiences a greater increase in output power than the second method. In the second method, more recoverable heat remains for the downstream cycle or a steam generator, if any.

Figure 4 The exergy destruction shares for (a) each cycle, (b) each component of system B (see online version for colours)

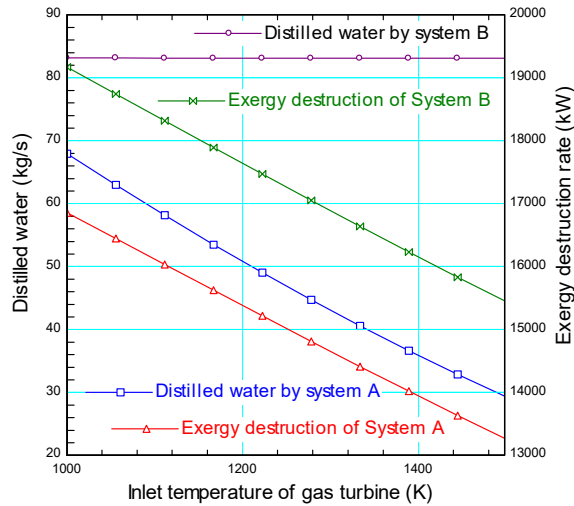


(a)

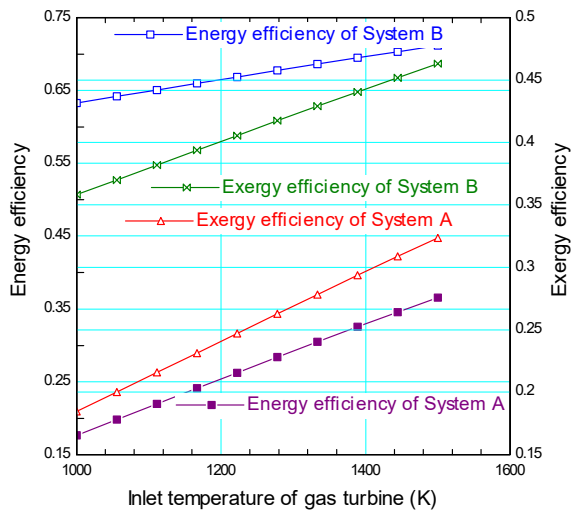


(b)

Figure 5 The effect of the gas turbine inlet temperature on (a) distilled water and exergy destruction rate, (b) energy and exergy efficiencies of proposed systems (see online version for colours)



(a)



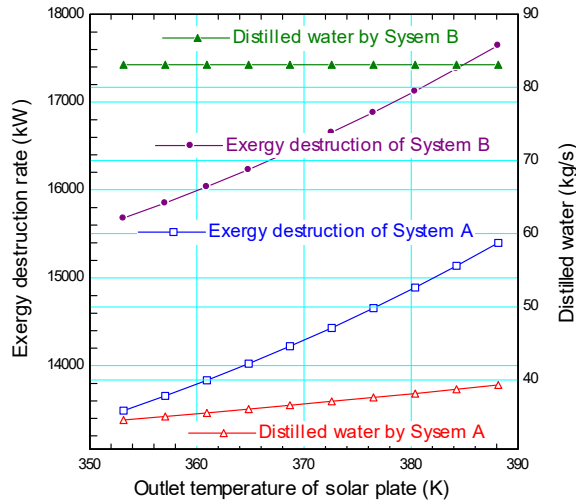
(b)

Following the intermediate state, in this work, the mass flow rate of biomass as well as the air coming from the compressor to the heater and gas turbine is constant. An increase in the inlet temperature of the GT requires more heat absorption by the air from the combustion gases in the air heater. So, the output power of the gas turbine increases and the temperature of the exhaust gases of the Brayton cycle and, thus, their harvestable energy decreases. This issue reduces the production capacity of the ORC in both systems.

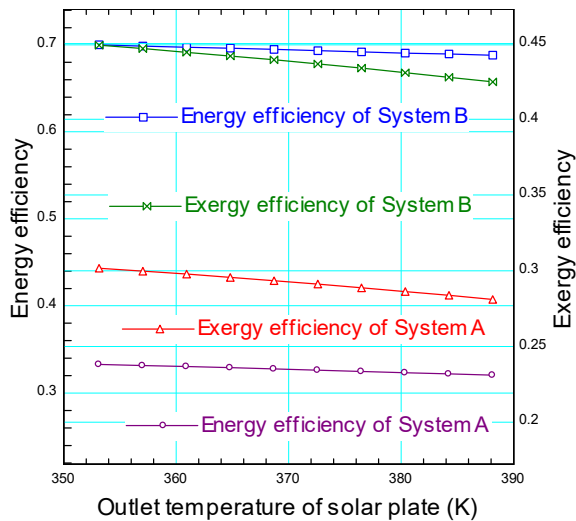
But because the increment of the gas turbine inlet temperature significantly raises its output power, the total net power of both systems increases. The noteworthy point is that the percentage increase in the power of system A is higher than that of system B; because more than 30% of the generated power of system B is provided by the geo turbine, whose changes are close to zero. Precisely for this reason, the amount of freshwater produced by system B remains unchanged with changes in the inlet temperature of the gas turbine. While reducing the power of the organic turbine means reducing the production of freshwater by system A because the high-pressure pump in this system takes its required power from this turbine. Figure 5(a) displays the effect of the GT inlet temperature on the amount of fresh water and the exergy destruction rate of systems. According to Figure 5(a), with the increase of T_6 , the exergy destruction of both systems diminishes. Increasing of T_6 is proportional to the reduction of the exergy destruction rate in the air heater and more effectively in the combustion chamber; which results in a reduction in the exergy destruction of the Brayton cycle. The exergy destruction of the ORC is also reduced in both systems due to the decrease in their output powers. Reducing the required area of the solar panel also means reducing the exergy degradation rate of the solar cycle in both systems. Figure 5(b) indicates that the energy/exergy efficiencies of two proposed systems. They are growing as the inlet temperature of the gas turbine increases. With a 50% increment of T_6 , the energy efficiency of systems A and B has increased by 107% and 12%, respectively, and their exergy efficiency has increased by 75% and 29%, respectively. It means that the effect of power growth is more significant than the effect of the distilled water reduction on the efficiency of two systems.

Figures 6(a) and 6(b) show the behaviour of the proposed systems in terms of the solar panel outlet temperature. The growth of T_{19} (T_{19} in system A and T_{21} in system B), which is the result of the larger area of the solar panel, causes more preheating of the ORC. As a result, the waste gases of Brayton will be able to heat more organic fluid in the evaporator. So, the ORC's output power of both systems increases. The water distilled by system A increases by 13.9% because its high-pressure pump depends on ORC's turbine and consumes more power. But there is not much change in the purified water by system B. The trend of changes in the amount of freshwater and the exergy destruction rate of the systems regarding to the outlet temperature of the solar panel can be seen in Figure 6(a). A 10% (Kelvin) increase in the solar panel outlet temperature due to the 212% rise in its area leads to an increase of more than 200% in the exergy destruction rate of the solar cycle in both systems. The exergy destruction of the organic Rankine cycle of both systems also increases slightly. But because the significant share of exergy destruction in both systems is related to the Brayton cycle and it is constant, the total exergy destruction of systems A and B increases by 14% and 12%, respectively. Figure 6(b) shows the changes in energy and exergy efficiencies versus the solar plate outlet temperature. With the increment of this temperature, despite the increase in power and purified water, the energy and exergy efficiencies of both systems decrease. Because the effect of the exergy destruction raising due to the increasing of the solar panel area on the efficiencies is more significant and reduces them. With a 10% (Kelvin) increase in panel output temperature, the energy efficiencies of offered systems A and B reduce by 3.75% and 1.7%, respectively, as well as, their exergy efficiencies decrease by 6.86% and 5.4%, respectively.

Figure 6 The effect of the solar plate outlet temperature on (a) distilled water and exergy destruction rate, (b) energy and exergy efficiencies of proposed systems (see online version for colours)



(a)

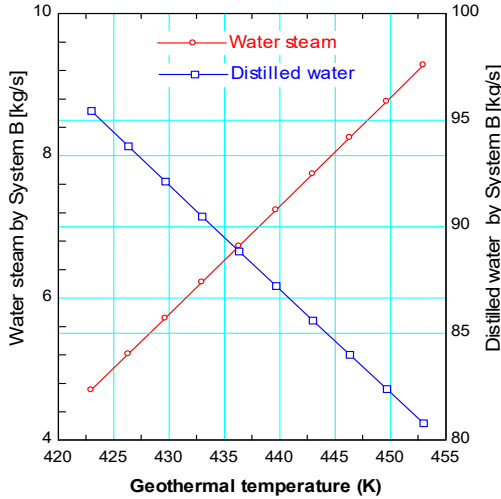


(b)

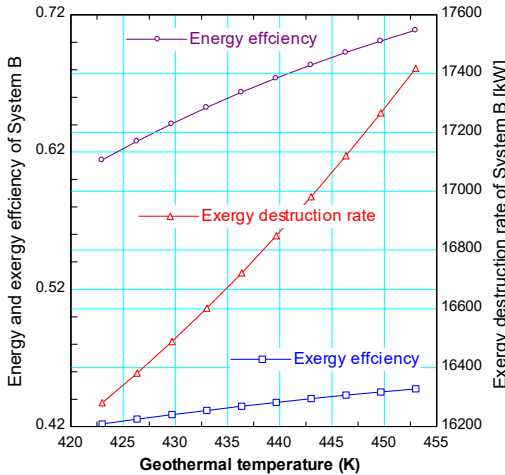
The influence of the geothermal fluid inlet temperature on the behaviour of the system B is depicted in Figures 7(a) and 7(b). It is clear that higher geothermal temperature provides more heat for the steam generator. A 7% increase in geothermal temperature results in a 97% increase in the water vapour production. Increasing the mass flow rate of water steam means much more heat absorption by water from the geothermal fluid in the steam generator; thus, the exiting temperature from the steam generator (inlet temperature of steam turbine) reduces. Therefore, the power production by this turbine, and consequently, the power consumption by the high-pressure pump of RO unit reduce. The

result is a 15.3% decrease in freshwater production due to a 7% increase in geothermal temperature. The large increase in the exergy destruction of the steam generator overcomes the decrease in the exergy destruction of the steam turbine and increases the exergy destruction of system B by 8%. Also, the dominance of the water vapour increasing over the decrease in the purified water and so raises the energy and exergy efficiency of system B by 15.4% and 6%, respectively, as visible in Figure 7(b).

Figure 7 The effect of geothermal temperature on (a) water steam and distilled water produced by system B, (b) energy and exergy efficiencies of system B (see online version for colours)



(a)



(b)

5 Conclusions

In this work, two multi-generation systems were proposed. In both, an organic Rankine cycle recovers the high temperature waste heat of a biomass-based gas turbine. System A is boosted by solar energy and system B by both solar and geothermal energies. Solar cycle of both systems has flat plate collectors. It is concluded that the low temperature solar cycle with flat plate collectors has low energy, about 4% of the biomass energy, which can only be used for ORC preheating and to produce higher solar temperatures, either the high area of the plates should be used or other types of collectors should be employed. On the other hand, the high-energy geothermal cycle, by 134% of the biomass input energy, is more suitable for strengthening the ORC, which is used for high-temperature heat recycling. Its energy is sufficient to employ a steam generator and a steam turbine in addition to reheating the organic Rankine cycle. Therefore, system B produces 34.6% more power and 132% more purified water than system A. It also produces 8.541 kg/s of water vapour, which is not possible for system A. These factors make system B have 111.3% and 49.32% higher energy and exergy efficiency, respectively. Exergy destruction of system B is 23.73% more. In addition, the RO desalination unit of system B is dependent on the steam turbine of the geothermal cycle, so changing the variables of the gas turbine and organic Rankine cycles does not change the fresh water produced by this system, while it affects the amount of purified water in system A.

5.1 Suggestions for the future work

- Environmental impact and exergo-economic analyses of the present work.
- Using other types of solar collectors like parabolic through collectors or solar dish collectors instead of flat plate collector.
- Employing of geothermal energy to regenerate the ORC instead of reheating it.

References

- Aghaziarati, Z. and Hajizadeh Aghdam, A. (2020) 'Thermoeconomic analysis of a novel combined cooling, heating and power system based on solar organic Rankine cycle and cascade refrigeration cycle', *Renewable Energy*, DOI: <https://doi.org/10.1016/j.renene.2020.10.106>.
- Alibaba, M., Pourdarbani, R., Khoshgoftar Manesh, M.H., Ochoa, G.V. and Duarte Forero, J. (2020) 'Thermodynamic, exergo-economic and exergo-environmental analysis of hybrid geothermal-solar power plant based on ORC cycle using emergy concept', *Heliyon*, Vol. 6, p.e03758, DOI: <https://doi.org/10.1016/j.heliyon.2020.e03758>.
- Altayib, K. and Dincer, I. (2022) 'Development of a geothermal-flash organic Rankine cycle-based combined system with solar heat upgrade', *Energy Conversion and Management*, Vol. 252, p.115120, DOI: <https://doi.org/10.1016/j.enconman.2021.115120>.
- Asgari, N., Khoshbakhti Saray, R. and Mirmasoumi, S. (2020) 'Energy and exergy analyses of a novel seasonal CCHP system driven by a gas turbine integrated with a biomass gasification unit and a LiBr-water absorption chiller', *Energy Conversion and Management*, Vol. 220, p.113096, DOI: <https://doi.org/10.1016/j.enconman.2020.113096>.
- Bellos, E., Tzivanidis, C. and Said, Z. (2021) 'Investigation and optimization of a solar-assisted pumped thermal energy storage system with flat plate collectors', *Energy Conversion and Management*, Vol. 237, p.114137, DOI: <https://doi.org/10.1016/j.enconman.2021.114137>.

- Bet Sarkis, R. and Zare, V. (2018) 'Proposal and analysis of two novel integrated configurations for hybrid solar-biomass power generation systems: thermodynamic and economic evaluation', *Energy Conversion and Management*, Vol. 160, pp.411–425, DOI: <https://doi.org/10.1016/j.enconman.2018.01.061>.
- Cao, Y.W.W., Mihardjo, L., Dahari, M. and Tlili, I. (2020) 'Waste heat from a biomass fueled gas turbine for power generation via an ORC or compressor inlet cooling via an absorption refrigeration cycle: a thermoeconomic comparison', *Applied Thermal Engineering*, Vol. 182, p.116117, DOI: <https://doi.org/10.1016/j.applthermaleng.2020.116117>.
- Cen, S., Li, K., Liu, Q. and Jiang, Y. (2021) 'Solar energy-based hydrogen production and post-firing in a biomass fueled gas turbine for power generation enhancement and carbon dioxide emission reduction', *Energy Conversion and Management*, Vol. 233, p.113941, DOI: <https://doi.org/10.1016/j.enconman.2021.113941>.
- Loni, R., Mahian, O., Markides, C.N., Bellos, E., Le Roux, W.G., Kasaeian, A., Najafi, G. and Rajaei, F. (2021) 'A review of solar-driven organic Rankine cycles: recent challenges and future outlook', *Renewable and Sustainable Energy Reviews*, Vol. 150, p.111410, DOI: <https://doi.org/10.1016/j.rser.2021.111410>.
- Mohammadi, M., Mahmoudan, A., Nojedehi, P., Hoseinzadeh, S., Fathal, M. and Astiaso Garcia, D. (2023) 'Thermo-economic assessment and optimization of a multigeneration system powered by geothermal and solar energy', *Applied Thermal Engineering*, Vol. 230, p.120656, DOI: <https://doi.org/10.1016/j.applthermaleng.2023.120656>.
- Musharavati, F., Khoshnevisan, A., Alirahmi, S.M., Ahmadi, P. and Khanmohammadi, S. (2022) 'Multi-objective optimization of a biomass gasification to generate electricity and desalinated water using Grey Wolf optimizer and artificial neural network', *Chemosphere*, Vol. 287, p.131980, DOI: <https://doi.org/10.1016/j.chemosphere.2021.131980>.
- Nafey, A.S. and Sharaf, M.A. (2010) 'Combined solar organic Rankine cycle with reverse osmosis desalination process: energy, exergy and cost evaluations', *Renewable Energy*, Vol. 35, No. 11, pp.2571–2580, DOI: <https://doi.org/10.1016/j.renene.2010.03.034>.
- Ochoa, G.V., Villicana Ortiz, E. and Duarte Forero, J. (2023) 'Thermo-economic and environmental optimization using PSO of solar organic Rankine cycle with flat plate solar collector', *Heliyon*, Vol. 9, No. 3, p.E13697, DOI: <https://doi.org/10.1016/j.helion.2023.e13697>.
- Pashapour, M., Jafarmadar, S. and Khalilarya, S. (2019) 'Exergy analysis of a novel combined system consisting of a gas turbine, an organic Rankine cycle and an absorption chiller to produce power, heat and cold', *International Journal of Engineering*, Vol. 32, No. 9, pp.1320–1326, DOI: <https://doi.org/10.5829/ije.2019.32.09c.13>.
- Pashapour, M., Jafarmadar, S. and Khalilarya, S. (2021) 'Energy, exergy and exergo-economic analyses of a novel three-generation system to produce power, heat and distilled water', *International Journal of Exergy*, Vol. 35, No. 4, pp.453–470, DOI: [10.1504/IJEX.2021.117051](https://doi.org/10.1504/IJEX.2021.117051).
- Zhang, W., Zhang, L., Chen, F., Cai, J., Liu, Y., Zhang, J., Wang, X. and Sohail, M. (2023) 'Multi-objective optimization and exergoeconomic analysis of solar and geothermal-based power and cooling system using zeotropic mixtures as the working fluid', *Process Safety and Environmental Protection*, Vol. 175, pp.495–515, DOI: <https://doi.org/10.1016/j.psep.2023.05.055>.